ARCHIVES
Of
FOUNDRY ENGINEERING
Published quarterly as the organ of the Foundry Commission of the Polish Academy of Sciences

ISSN (1897-3310)
Volume 11
Special Issue
2/2011
53–58

11/2

Description of selected structural elements of composite foams using statistical methods

K. Gawdzińska[a], J. Grabian[a], Z. Pędzich[b], W. Przetakiewicz[a],

[a] Institute of Basic Technical Sciences, Maritime University of Szczecin, ul. Podgórna 51/53, 70-205 Szczecin, Poland
[b] Department of Advanced Ceramics, AGH – University of Science and Technology, Av. Mickiewicza 30, 30-059 Krakow, Poland
e-mail: k.gawdzinska@am.szczecin.pl

Received 11.04.2011; Approved for print on: 26.04.2011

Abstract
This article makes use of images from a computer tomograph for the description of selected structure elements of metal and composite foams by means of statistical methods. Besides, compression stress of the tested materials has been determined.

Key words: composite foams, tomography, statistics.

1. Introduction

Forecasts concerning the development of technologies and applications of new materials in machine construction indicate that metal cellular materials are gaining an increasing range of applications in machine construction, particularly in transport facilities [1–5]. The commercial trend connected with the projected dynamic growth of applications of these materials is shown in Figure 1.

Cellular structures have a number of unique properties that are crucial for their choice in machine construction. Their low density makes them an ideal filling material for layered structures. Low thermal conductivity is vital for their use as insulating material, while the ability to suppress sounds offers new applications as soundproof linings.

On the other hand, the susceptability of these materials to substantial deformation under relatively small loads may be used in packings, in systems for energy absorbtion or explosion effect reduction. Properties of cellular materials include both isotropy and anisotropy [3, 5–10]. Apart from natural cellular materials, such as bark, wood, bones etc., man-made products of this type include well-known and widely used materials: pumice, cellular concrete or foamed polymers, used in shock absorbers, packaging or construction elements, to name just a few applications. Metal foams also belong to cellular materials, gaining an increasingly wider range of use. To a large extent their properties are determined by porosity (size of gas bubbles). The internal structure of metal foams is shown in Figure 2, while Figure 3 displays foams of varied size of gas bubbles, or pores. The size of pores and type of material significantly affect the quality of these materials [9–13].

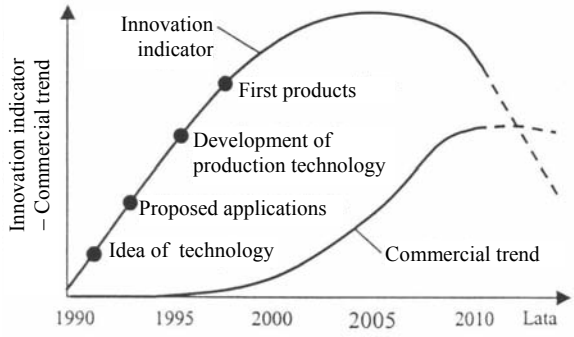

Fig. 1. Forecast of cellular structures applications in machine construction [2]

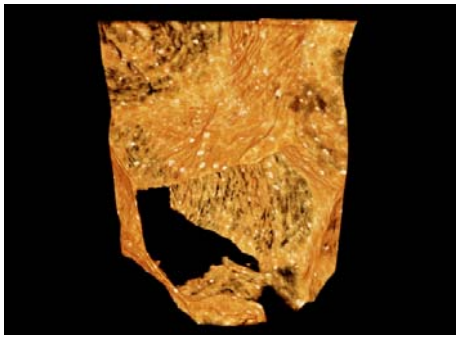

Fig 2. A 3D image of metal composite foam

It is important to be able affect selected parameters of the structure through technological process control, which will enhance the quality of composite materials under examination [3, 7]. This work identifies the sphericity and pore diameters in selected materials by methods of descriptive statistics. Selected foams were also subjected to compressive loads in order to check how the size of pores (bubbles) affects the material stress.

2. Research

Tests of four types of foams are descussed in this work. Three randomly chosen samples were taken from each group, and the results were averaged. The four samples were made of different materials: type H foam was made of aluminium alloy AlSi, while the foams of type A, B and C – composite foams with an AlSi9 matrix and SiC reinforcement phase with a 15% weight fraction – differing in pore size (see Figure 3). The tested materials were made at the Materials Engineering Department, Maritime University of Szczecin, by blowing gas into liquid metal [7–10].

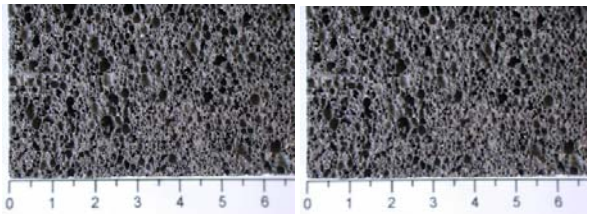

H A

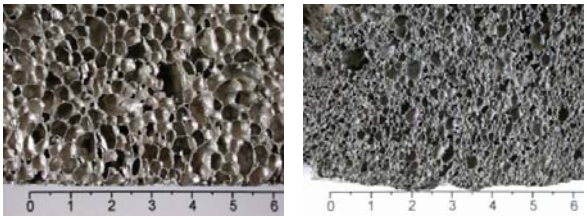

B C

Fig.3. Metal foams with varying pore sizes, used for tests described in this work (for notations see the text)

Statistical analysis was carried out in order to describe the pores in the examined materials. The analysis took into consideration two variable parameters to be identified in two groups of foams: type H and types A, B, C. These parameters are:

– sphericity percentage (understood as the degree of pore shape to which it resembles a sphere), and
– mean diameter in μm.

The data used for the description of bubbles (i.e. pores) were obtained from tomographic images (Fig. 4) using a MicroXCT device made by Xradia (USA). The images were processed by means of the Aphelion program for computer-aided image analysis and the Statistica 9.0 software.

The tested materials underwent compressive tests using a strength machine, model H10K-T.

Analysis of the sphericity variable ‘

Basic statistical parameters for the sphericity variable with the mean values and the values for each type of sample are given in Table 1.

Table 1.
Statistical parameters of the sphericity

Spheri-city	Mean	Median	Mini-mum	Maxi-mum	Standard deviation	Variance coefficient
All types	72%	74%	21%	99%	16%	22.92%
type H	71%	74%	26%	92%	16%	23.08%
type A	74%	77%	23%	99%	17%	22.50%
type B	67%	68%	29%	93%	14%	21.42%
type C	67%	69%	21%	97%	15%	22.82%

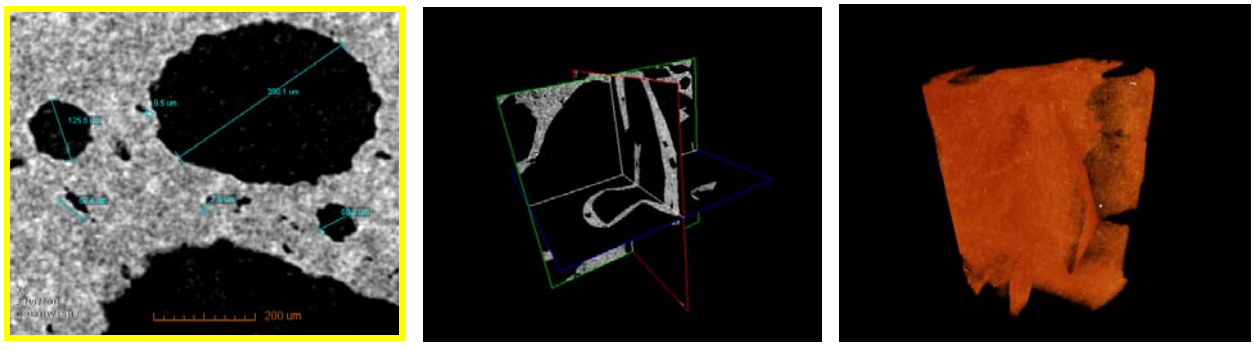

Fig. 4. Examples of composite foam images used for analysis – computer tomography

The mean values of sphericity oscillate around 70 %, while the median for each type of sample is higher than the mean by 2% – 3%. The sphericity values belong to the interval from 21% to 99 %. The values of standard deviations of this variable range from 14% to 17%, which makes up approximately 22 % of the mean value.

The boxplots (box and whiskers plots) below [14–15] show the scatter of the sphericity variable relative to the median, comparing the sphericities for each type of foam with the foam made of aluminium – type H (Fig. 5–7).

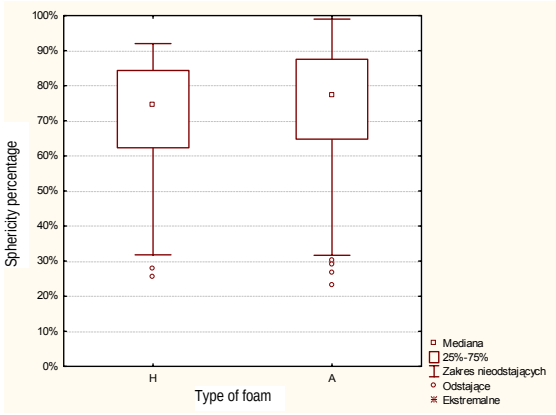

Fig. 5. A boxplot for the sphericity variable of type H and A foams

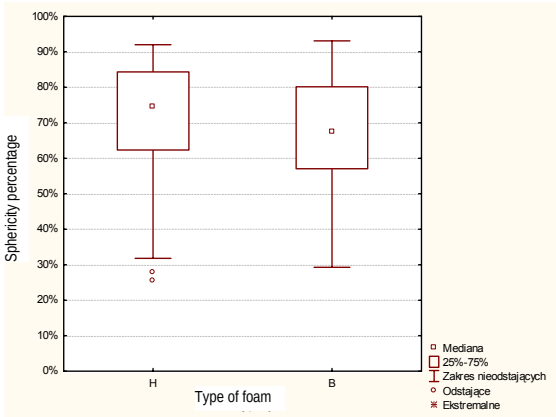

Fig.6. A boxplot for the sphericity variable of type H and B foams

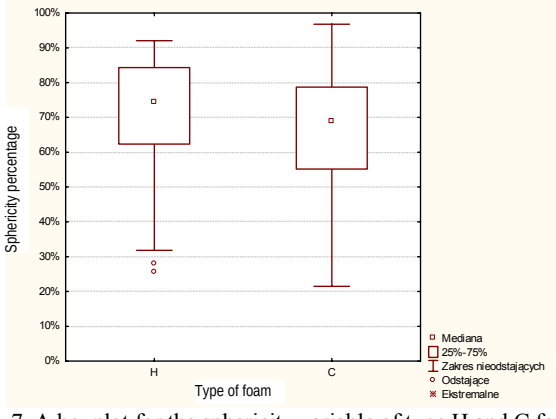

Fig. 7. A boxplot for the sphericity variable of type H and C foams

Comparing the distribution of the measures of central tendency (median and quartiles) of the sphericity for each foam type with the H type foam (Figures 5–7), one will see that the type A foam has a distribution of the sphericity position measures most similar to the foam H. The foams B and C have a different distribution of the median and quartiles of the sphericity than the foam H.

On the other hand, if we make a simultaneous comparison of the sphericity variable of all foam types (Fig. 8) we will note that the greatest median value is that of type A foam pores sphericity, while the smallest median value is that of sphericity in the type C foam pores. The greatest scatter of the sphericity variable around the median is found for type C foam . The sphericity vaiable assumes outlying (untypical) values for type A and type H foams, while type B and C foams feature values of sphericity that belong to the typical range.

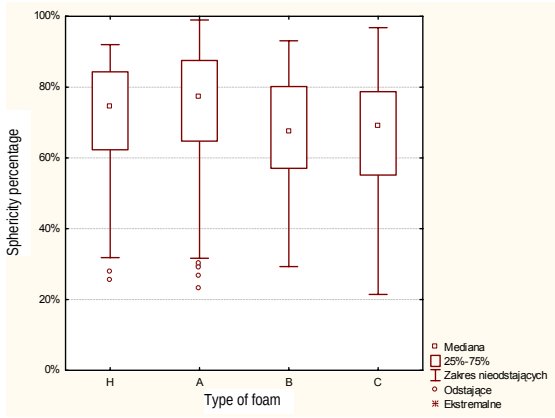

Fig. 8. A boxplot for the sphericity variable for each type of foam

The sphericity dispersion relative to the mean value for each type of foam is shown in Figure 9.

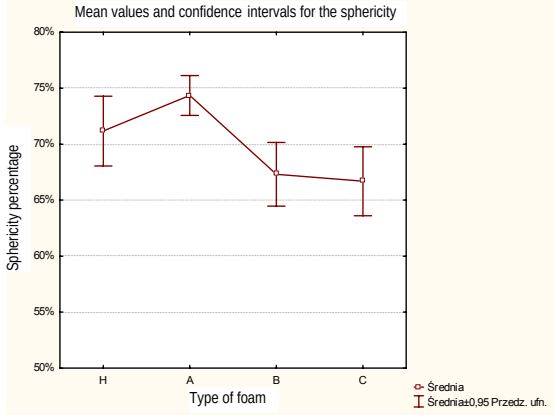

Fig. 9. Mean values and confidence intervals for the sphericity for each type of foam

It follows from the diagram that the type A foam has the greatest mean value, and the smallest mean value of sphericity characterizes the type C foam. The smallest scatter around the sphericity variable is observed for the type A foam. The sphericity

variable for type H, B and C foams shows a comparable scatter around the mean value.

Figure 10 presents a histogram of the sphericity variable with no division made into foam types.

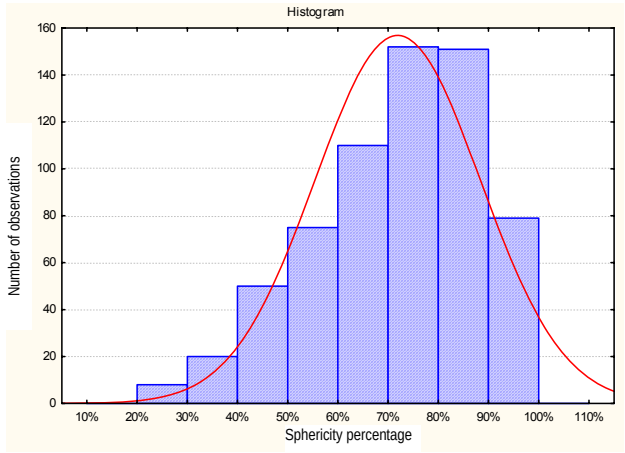

Fig. 10. An overall histogram of the sphericity variable

It will be noted that the sphericity variable has a distribution close to the normal distribution $N(0.71; 0.16)$, where 0.71 is the mean value of the sphericity, and 0.16 is the standard deviation for this variable. The distribution has a left-hand assymetry, i.e. more samples have the sphericity above the mean value.

The histograms, made to illustrate the sphericity for each type of foam, are shown in Figure 11.

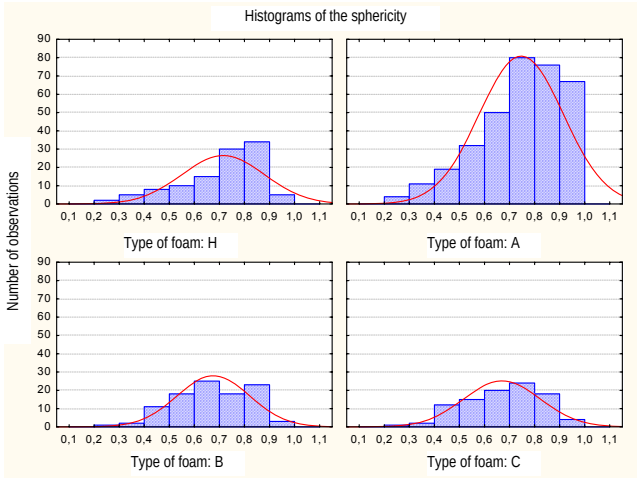

Fig. 11. Histograms of the sphericity for each type of foam

The analysis of these histograms reveals that for all types of foam the sphericity variable features a distribution similar to normal distribution $N(\mu,\sigma)$, where μ is the mean value, and σ is the standard deviation. The values given the brackets confirm the above conclusion that the sphericity of pores in each foam has normal distribution and are equal to: type H - $N(0.71; 0.16)$, type A - $N(0.74; 0.16)$, type B $N(0.67; 0.14)$ and type C $N(0.66; 0.15)$.

In foams of type H and A the distribution of sphericity has a left-handed asymmetry, that is more samples in these foams have sphericity above the mean value, while foams of type B and C have a symmetrical distribution of the sphericity variable.

Analysis of the mean diameter variable

The foams of type H and types A–C were also compared in terms of the mean diameter variable. The graph below (Figure 12) includes the median, quartiles, and scatter (of this variable of foam.

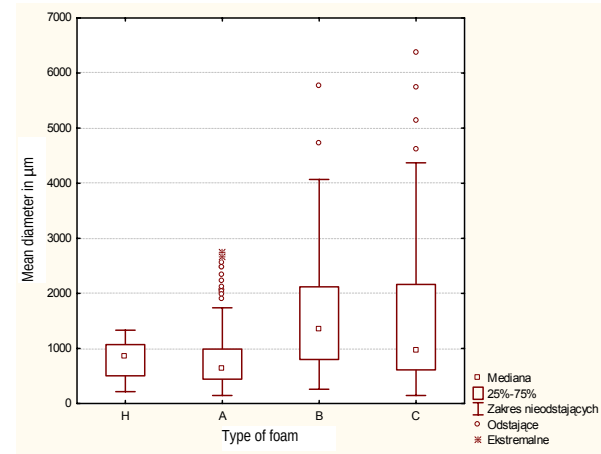

Fig. 12. A boxplot of the mean diameter variable for each type of tested foam

It follows from the boxplot above that foams H and A have the smallest median of the mean diameter, and foam B has the largest median. Besides, the mean diameter variable for foams of H and A type shows a smaller scatter than foams B and C, although foam A features outlying values, that is those beyond the 25%–75% range of the median, while foam H does not have pore diameters with outlying values.

Strength tests

The foams under consideration were tested for compressive strength (samples of the same dimensions). The results are given in Figure 13.

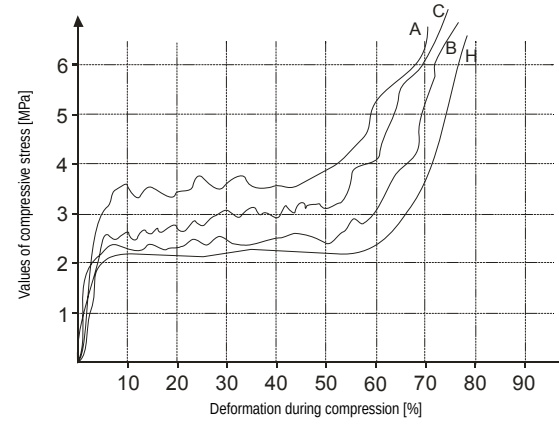

Fig. 13. Relationships between values of compressive stress and deformation for foams H and A-C

Analyzing the data presented in Figure 13 we should account for the fact that these foams were of different density. Foam H had a density 0.228 g/cm^3, while composite foams, respectively: A – 0.455; B – 0.250; C – 0.301 g/cm^3. If we assume that the true density of AlSi9 alloy is 2.65 g/cm^3, and the density of SiC is 3.21 g/cm^3, the calculated true density of the composite used for foams was 2.72 g/cm^3. Using these data, we can calculate the apparent densities and porosities of all tested foams. The calculation results are collected in Table 2.

Table 2.
Densities and porosities of the tested materials

Material (foam)	Apparent density, g/cm^3	True density, g/cm^3	Relative density, % theoret.	Porosity, %
H	0.228	2.65	8.60	91.60
A	0.455	2.72	16.73	83.27
B	0.250	2.72	9.19	90.81
C	0.301	2.72	11.07	88.93

Therefore, the tested samples differed not only in pore size but in average porosity as well, which must have affected the results of strength tests. However, analyzing the curves of relationship between the stress and deformation recorded during the tests, we can make a qualitative comparison between the materials. All recorded curves generally run similarly, and three stages can be disinguished in the process of destruction of foam microstructures during the test. The first stage comprising a single-figure percentage of deformation corresponds to the range where the stress-deformation relationship is linear. Then the scale of deformation includes some fifty percent deformation where the mean stress remains more or less the same or grows slightly. In the final stage where a substantial deformation already exists (above 50 – 60%) the stress sharply rises with insignificant changes in deformation.

The values of stress read out from the analyzed curves (Figure 13) clearly show that the lower overall porosity is, the higher is the stress needed for deformation to take place. However, another difference may be observed between the curve for the alloy and the curves for the composites – the alloy curve in the second stage is relatively 'smooth', while those for composite materials reflect significant fluctuations of the stress values. This is most probably related with the detrimental effect of carbide intrusions that modify the plastic deformation in metal. The detailed analysis of the phenomen calls for further investigation. At this point of research we can only state that the amplitude of the fluctuations depends on foam density: the higher the density, the larger fluctuations of stress during deformation.

3. Summary

It follows from the above statistical analysis that all examined materials have pores, i.e. gas bubbles that roughly resemble spheres so that their sphericity can be statistically determined (Table 1 Figures 5–11). The type H and A foams feature bubbles whose sphericity (Fig. 5) and diameters (Fig. 12) are similar.

The strength of composite foams is higher than that of an alloy foam (Fig. 13). This is related with the presence of the reinforcement phase as well as the density and porosity of foams. Of the composite foams, type A foam has the highest compressive strength due to its smallest pores and highest density. The type C foam, in turn, has the microstructure with pores of much diversified size (Figures 3 and 12). The type B foam, with the lowest strength of all tested composite foams (Fig. 13), has the largest pores and lowest density (Tables 1 and 2), and in this respect resembles the alloy foam most.

The foam deformation in the compression test shows a difference between the behaviour of the AlSi9 alloy foam and composite foams. In the latter the presence of carbide intrusions brings about fluctuations on the stress-deformation curve due to local cumulation of stresses.

The use of tomographic images [16] may contribute to a better, more complete description of shape depicted in 3D space of the examined materials. With no need to apply destructive tests (Fig. 4), in this approach the sample can be easily described by statistical methods.

Acknowledgements

Authors are very grateful to Prof. S. H. Lau for assistance in metallic foams investigation using Xradia MicroXCT equipment.

The work was supported by the Polish Ministry of Science and Higher Education under AGH project 11.11.160.364. and project N R07 0017 06.

Literature

[1] T.W. Clyne, F. Simancik, Metal MatriX Compositea and Metalic Foams, Euromat- Volume 5.WILEY-VCH Verlag, Weinheeim 2000.
[2] C. Körner, R.F. Singer, Processing of Metal Foams – Challenges and Opportunities, Metal Matrix Composities and Metallic Foams Euromat, Vol. 5, 3–13.
[3] E. Koza, M. Leonowicz, S. Wojciechowski, Analiza strukturalna pian aluminiowych. Polskie Towarzystwo Materiałów Kompozytowych, Kompozyty, 1999.
[4] J. Baumeister, J. Bauhart, M. Weber, German Patent DE 4426627, 1997.
[5] T. Miyoski, Aluminium Foam „ALPORAS". The Production Process, Properties and Applications. Sympozjum MRS, vol.521, San Francisco, 1998
[6] P. Asholt, Manufacturing of Aluminium Foams from PMMC Melts – Material Characteristics and Typical Properties, in Metallschäume, Banhart J. (ed.), Bremen, Germany, MIT Publishing 1977, 27–37.
[7] K.M. Hurysk, et. al., Steel and Titanium Hollow Sphere Foams, MRS Symposium Proceeding, Vol. 521, San Francisco, 1998, 191–204.
[8] T. Miyoshi, et. al., Aluminium Foam, "ALPORAS": The Production Process, Properties and Applications, MRS Symposium Proceeding, Vol. 521, San Francisco, 1998, 132–138.
[9] E. Koza, M. Leonowicz, S. Wójcikowski, Analiza strukturalna pian aluminiowych, Kompozyty 2 (2002) 289–231.

[10] J. Banhart, J. Baumeister, Production Methods for Metallic Foams, MRS Symposium Proceeding, Vol. 521, 121–132.
[11] J.T. Wood, Production and Applications of Continuously Cast, Foamed Aluminium, Proceeding of the Fraunhofer USA Metal Foam Symposium, October 7–8, Stanton Delaware, 1977, 1–5.
[12] J. Sobczak, Piany metalowe monolityczne i kompozytowe oraz gazary. Instytut Odlewnictwa, Kraków 1998
[13] Hull D., Clune T.W., An Introduction to Composite Materials, Cambridge University Press 1996.
[14] K. Chmielewski, S. Berczyński Statystyka matematyczna. Ćwiczenia laboratoryjne z wykorzystaniem pakietu STATISTICA PL, Wydawnictwo Uczelniane- Politechnika Szczecińska, Szczecin 2002.
[15] C. Domański, Testy statystyczne, PWE, Warszawa 1999.
[16] E. Maire, E. Watterbled, J.Y. Buffiere, G. Peix, Deformation of a Metallic Foam studied by X-Ray computed Tomography and Finite Element Calculations, Metal Matrix Composites and Metallic Foams Euromat, Vol. 5, 68–73.